Constraints on the nature of Siljan as an impact structure

Richard A.F. Grieve

Department of Energy, Mines & Resources
Earth Physics Branch
Gravity, Geothermics & Geodynamics Division
1 Observatory Crescent
Ottawa, Ontario
K1A 0Y3

Internal Report 84-15

Submitted to: Vattenfall Deep Gas Project
September 1984

INTRODUCTION

The Siljan ring structure has a 32 km diameter central core of Dala granites of Sub-Jotnian age surrounded by a 45 km diameter annular depression, which is partially filled with lakes and contains down-faulted Ordovician and Silurian sediments (Fig. 1). The characteristic ring form, the presence of shatter cones, allochthonous breccias, breccia and impact melt dikes and microscopic, shock planar features in the central granites provide abundant evidence that Siljan is a large, eroded impact structure (Rondot, 1975; Svensson, 1971, 1973). Isotopic dating of impact melt rocks place the age of the impact event at 326 ± 1 my (Bottomley *et al*., 1978) and the original, pre-erosional diameter of the structure is estimated to have been approximately 52 km (Grieve, 1982).

Current understanding of the formational processes in impact cratering events comes from the geologic and geophysical character of terrestrial impact structures, studies of the morphometric parameters of fresh lunar and planetary craters, small-scale experimental and high-energy explosion craters, numerical simulations using continuum-mechanical cratering codes, and theoretical considerations. These studies, particularly those at terrestrial craters, provide a considerable base of knowledge from which to constrain the nature of the Siljan structure. Following some general background with respect to cratering processes, this contribution considers some of the characteristics of an impact structure such as Siljan which may be of relevance to the Deep Gas Project of the Swedish State Power Board (Vattenfall).

BACKGROUND

Approximately 100 terrestrial impact structures ranging in size from a few tens of meters to 140 km are currently known (Grieve, 1982). Observational data on terrestrial impact structures can be found in papers dealing with individual structures and in such compilations as French and Short (1968), Masaitis et al. (1980), and Roddy et al. (1977). The terrestrial population follows the morphological progression with size which is exhibited on other planetary bodies. Smaller craters are essentially a simple, bowl-shaped depression partially filled by breccias, while larger structures have a complex form with uplifted material in the form of a central peak and/or ring surrounded by a complexly faulted annulus and rim area. These complex structures have a relatively shallower depth/diameter ratio than simple craters and occur at diameters greater than 4 km in crystalline rocks on earth (Dence et al., 1977). Detailed analyses of the stages of the cratering process can be found in such papers as Gault et al. (1968), Dence et al. (1977), Croft (1979, 1980), Grieve et al. (1977, 1981) and others and need not be repeated. The concern here is with some general background and terminology of impact phenomena that will allow Siljan to be placed in the context of a terrestrial complex impact structure.

On impact, kinetic energy is transferred from the projectile to the target rocks by means of a hemispherically propagating shock wave, which increases the internal energy and imparts kinetic energy to the target. Depending on impact conditions: impact velocity, physical properties of projectile and target, peak pressures are in the megabar to tens of megabar range and associated post-shock temperatures close to the point of impact are above the vaporization temperature of silicates. Particle motions induced in the target by the shock and subsequent release or rarefaction waves produce a "cratering flow field" in the target materials. This flow field has two components.

Outwards and upwards particle motions excavate target material by ballistic ejection, resulting in an excavated cavity of depth d_e and diameter D_e. As the cavity grows by excavation, the second component of the flow-field, which involves the volume immediately under the impact point, leads to the downward and radial displacement of autochthonous target material, thereby enlarging the cavity. This combination of excavation and displacement defines a transient cavity, which is two to three times deeper than the excavated cavity (Dence et al., 1977). As the name indicates this transient cavity does not survive throughout the entire cratering process. Modification processes operate subsequent to, or possibly even during transient cavity growth, and serve to shallow the transient cavity and bring it to some equilibrium form.

In simple craters, the displacements induced in forming the transient cavity floor are almost entirely "locked-in" and modification is by wall failure. This is not the case for larger, complex structures. In complex structures, the transient cavity floor undergoes uplift and the rim area collapses downward (Fig. 2). Although not fully understood, this extensive modification appears to be initiated under plastic failure conditions in which the rocks have little or no yield strength. Various suggestions for producing conditions equivalent to this hydrodynamic response of the target rocks include: crushing, and/or shearing, and/or frictional melting between blocks and acoustic fluidization. The driving mechanism for uplift is generally considered to be elastic rebound of the transient cavity floor, in combination with the release of gravitational potential energy from the original overheightened transient cavity rim area. Further details of the formation of complex crater-forms can be found in papers in Schultz and Merrill (1981). It is sufficient to note that in the case of a structure such as Siljan, the central Dala granites represent the eroded remanent of the uplifted transient cavity floor and that the Paleozoic sediments were outside the original area of deep-seated excavation and owe their preservation to down-faulting accompanying the collapse of the transient cavity rim area during modification.

A number of inferences and parameters of the Siljan structure, based on the present understanding of large-scale terrestrial impact events, are given below.

ENERGY ESTIMATE, SHOCK HEATING

Energy-diameter scaling relationships for relatively simple craters are the subject of recent review (Grieve and Cintala, 1981; Holsapple and Schmidt, 1982). The problems with determining precise scaling relations are compounded considerably when considering complex structures in the size range of tens of kilometers which have undergone considerable post-excavation modification. Scaling relations for complex structures have the form:

$$D = F\ E^{1/\alpha} \qquad (1)$$

where D is final diameter, F is a function of parameters such as impact velocity, target and projectile density, gravity, and target strength; E is kinetic energy; and α is an exponent with a range of estimates of from 3.4 to 4.0. As with most structures, the impact parameters are virtually unknown for the Siljan event. Based on a number of observations, Dence et al. (1977), however, have determined an empirical scaling relation for complex terrestrial craters where:

$$D = 1.96 \times 10^{-5}\ E^{1/3.4} \qquad (2)$$

and D is in km and E in Joules. For a diameter of 52 km, this relation gives an estimated kinetic energy of 1.4×10^{22}J for Siljan, approximately an order of magnitude greater than the annual output of internal energy of the earth.

This should probably be regarded as a minimum estimate, as the Dence et al. (1977) relation does not fully account for energy losses accompanying vaporization and superheating of impact melt rocks.

Although it is theoretically possible to differentiate the velocity and mass components of such an energy estimate (Grieve and Cintala, 1981), the basic observational data are lacking for Siljan. As impact velocity and projectile type and size control peak pressures and temperatures, as well as radial distance to a given shock isobar or post-shock isotherm, only general statements can be made about the pressure-temperature distribution at Siljan. For illustration, it has been assumed that the Siljan event was the result of the impact of a chondritic body impacting granite at 25 km s^{-1}, the r.m.s. impact velocity of Apollo bodies (Shoemaker, 1977). For a spherical body with a density of 3000 kg m^{-3}, the diameter of the projectile would be on the order of 3 km. Energy partitioning calculations for a 3 km diameter chondritic projectile impacting granite at 25 km s^{-1} indicate that 65% of the projectile kinetic energy will be partitioned into waste heat in the target (Cintala and Grieve, 1984).

Most of this waste heat is concentrated close to the point of impact, where it results in the melting and vaporization of approximately 500 km^3 of the target rocks. Although some of the melted and vaporized material will be ejected from the growing cavity by the cratering flow field, some will remain to form an annular melt sheet in the centre of the final crater (Grieve, et al. 1977). This sheet, with an initial temperature on the order of ~ 2200°C, may have originally been ~ 200 m thick at Siljan and essentially covered the center of the final structure extending out to the area of the Paleozoic sediments. There is insufficient data, however, to determine whether it originally covered some of the Paleozoic sediments and produced local thermal metamorphic effects. Such a thickness of impact melt would require on the order of 1000 - 2000 y to crystallize completely (Onorato et al., 1978) and perhaps 10,000 y to cool completely to ambient temperature.

Post-shock temperatures associated with release from shock compression attenuate relatively rapidly from the point of impact (Grieve and Cintala, 1981; Cintala, 1984) Peak pressures recorded in rocks at the center of central uplifts at terrestrial complex craters are generally in the 25-30 GPa range, corresponding to post-shock temperatures of 100-200°C. At the transient cavity rim, now corresponding approximately to the area of Paleozoic sediments, pressures were more likely in 0.5 - 1.0 GPa range, with little or no associated post-shock heating.

ESTIMATES OF EXTENT OF EXCAVATION AND UPLIFT

The depth of excavation at complex structures is the subject of some debate (see papers in Schultz and Merrill, 1981). There is, however, a general consensus that it is not proportionally greater than that experienced in smaller simple craters. Empirical data from code-calculations of nuclear explosions and experimental impacts place the maximum depth of excavation d_e for small craters at:

$$d_e = 0.1\ D_e \qquad (3)$$

where D_e is the diameter of the excavated cavity and is equivalent to the diameter of the transient cavity at the original ground surface (Croft, 1980; Grieve and Garvin 1984). Due to the considerable amount of post-excavation modification, some uncertainty, however, rests with estimating D_e at complex structures. From stratigraphic data at complex structures in sedimentary targets (Fig. 3), the relative position of near surface sediments (such as the Paleozoic sediments at Siljan) and the limit of diagnostic shock effects, Grieve et al. (1981) estimate that:

$$D_e = 0.5 - 0.65\ D \qquad (4)$$

where D is the final rim diameter at complex structures. A more recent compilation of data by Croft (1984), which includes data on central uplifts at lunar craters, suggests the following empirical relationship for terrestrial complex structures:

$$D_e = 1.23\ D^{0.85}. \qquad (5)$$

For Siljan with D = 52 km, equation (4) results in a D_e estimate of 26 - 34 km, whereas relation (5) gives 35 km. On the basis of (3), this gives a maximum depth of excavation for Siljan of 2.6 - 3.5 km.

An alternative measure of the depth of excavation is the amount of stratigraphic uplift undergone by the central rocks (Fig. 3), the argument being that, at least in fresh craters, higher stratigraphic units now absent from the central uplift were removed largely by excavation. Observational data on the amount of stratigraphic uplift, which is defined as the observed amount of uplift undergone by the deepest marker horizon now exposed at the center of a complex structure, at a number of terrestrial structures results in the empirical relationship:

$$SU = 0.06D^{1.1} \qquad (6)$$

where SU is stratigraphic uplift and D is final rim diameter (Fig. 4; Grieve et al., 1981). The calculated value for SU at Siljan is, therefore, 4.6 km. As a depth of excavation estimate, this is somewhat in excess of that determined earlier. Given the uncertainty in the data used to define the above empirical relations, however, this is not considered to be a major discrepancy, particularly as the SU relation is defined by only two data points above a diameter of ~ 25 km (Fig. 4; Grieve et al., 1981).

EXTENT OF FRACTURING

Considerable brecciation and fracturing accompanies crater formation and is evidenced generally by the occurrence of a gravity low over impact structures. Although often complicated by regional gradients and local density contrasts, the common gravity signature of both terrestrial and lunar complex impact structures is an outer negative ring beginning in the general area of the original rim area which then grades upwards in value towards the center (Fig. 5; Dvorak and Phillips, 1977; Sweeney, 1978; Barlow, 1979). This outer negative ring can be attributed to increased fracture porosity in the area of downfaulting in the rim area. The central portion of the residual gravity field over complex structures is still generally negative, with respect to the regional field, also indicating increased fracturing. The fact that it is higher than the outer negative ring can be best explained by a relative reduction in fracture porosity due to the nature of the uplift process, where the uplift trajectories are upwards and inwards. This results in a relatively compressive regime, with closing of some of the fractures, in the final central uplifted volume. For example, the peripheral gravity low at the Manicouagan structure can be modelled with a density contrast of -130 kg cm^{-3}, which corresponds to a fracture porosity of 5-10%, depending on whether the fractures are water-filled or not. By comparison the central uplift area has little or no density contrast, with a residual anomaly of 0 mGal (Fig. 5a and b; Sweeney, 1978).

The residual gravity signature of Siljan (unpublished data; this report) is apparently more complex than that of many other complex structures. The presence of a gravity low in the east and south, in the area between Boda and

Rattvik, appears consistent, however, with the above generalizations. The concentric low in the north is centered over Skattungen in the area of the down-dropped sediments (Fig. 1). Its concentric nature, however, suggests that its ultimate cause goes beyond simple induced fracture porosity and may be related to sub-surface rock-type contrasts. It may well reflect the occurrence of the northerly Siljan granite, which is relatively less dense, 2604 kg m^{-3}, compared to other granites in the area, 2668 kg m^{-3} (unpublished data, this report).

A zone or halo of increased fracturing can be observed surrounding some terrestrial craters. The fracture zone can be considered to be that volume which was stressed above the inherent dynamic strength of the target rocks. One of the few quantitative analyses of increased fracture density has been undertaken by Gurov and Gurova (1981), who suggest that fracturing decays as R^{-3}, where R is radial distance from the crater center. They indicate that increased fracturing extends for approximately one crater diameter beyond the relatively fresh 23 km diameter, 3.5 $\pm$ 0.5 my old, Elgygytgyn structure in Siberia. Similar-sized fracture haloes can be observed on LANDSAT images of more deeply eroded structures such as Manicouagan (Dence, 1977; Grieve and Head, 1983) and Clearwater (Dence _et al_., 1977) in the Canadian Shield. In the case of Siljan, therefore, increased fracturing is expected to have occurred out for a distance of approximately 50 km beyond the original rim.

Drilling and reflection seismic profiles indicate that _major_ structural disturbance beneath complex impact structures extends in the center to a _maximum_ depth of approximately 1.5SU (Fig. 3; Brennan _et al_., 1976; Brown, 1973). It involves a roughly paraboloid volume extending upwards, as expected, to the surface limit of obvious structural uplift and modification. At Siljan, therefore, the depth of major structural disturbance is expected to have originally extended to a depth of approximately 7 km.

Tensile fractures will extend beyond this depth and will occur down to the depth where the lithostatic pressure exceeds the strength of the rarefaction wave which would produce tensile failure at zero confining pressure (Grieve and Robertson, 1984). The dynamic tensile strength of crustal rocks rarely exceeds 0.04 GPa (Grady and Hollenbach, 1979). A first order calculation, based on a 3 km chondritic projectile impacting granite at 25 km s^{-1} and the shock wave attenuation model of Cintala (1984), indicates that impact-induced fracturing in the center of Siljan could occur to depths on the order of 35-40 km. In the calculation, it was assumed that the tensile stress associated with the rarefaction wave was equal in magnitude to that of the shock wave at any given radial distance. Thus the Siljan impact event had the potential to initially fracture, at least in the center, the entire crustal column. It is expected, however, that many of these initial fractures will close by compaction and heal due to mineral percipitation. Although it has been generally assumed that pore space is virtually eliminated at depths greater than 8 km due to lithostatic pressure (Perrier and Quiblier, 1974), the recent results of the Kola drill hole indicate that circulating fluids in fracture zones exist at greater depths (Koglovsky, 1982). Therefore, whether or not some of the initial, deep crustal fracturing beneath the Siljan could remain open is an unanswered question.

EROSION ESTIMATE

The original topographic relief of the Siljan structure has been removed by erosion and the sub-structure of the crater floor exposed. Although there is considerable scatter in the depth-diameter relationship for terrestrial complex structures, it appears to conform to:

$$d = 0.5\ D^{0.3} \qquad (7)$$

where d is original, pre-erosional depth to the autochthonous rocks of the crater floor (Grieve, 1984). This requires approximately 1.5 km of erosion to remove the topographic rim and expose the crater floor at Siljan. It does not necessarily mean, however, that 1.5 km of erosion has occurred throughout the entire Siljan area, e.g. in the area of the down-dropped Paleozoic sediments. The absence of any expression of a central positive topographic feature such as a peak and/or rings, as well as the removal of any annular melt sheet, suggest at least 1 km of erosion in the center (Fig. 4). It should be noted, however, that the original physical heights of central features (Fig. 4) are even less well-constrained than depths estimates. This estimate of 1 km is a minimum, as the peak recorded pressures in the exposed center are on the order of 12 GPa, based on the occurrence of $(10\bar{1}3)$ planar features in quartz grains (Svensson, 1973). This is lower than the expected 25-30 GPa at the center of terrestrial complex structures and is indicative of erosion to below the original autochthonous crater floor.

SUMMARY

The preceding discussion has presented a number of observations regarding the original and present nature of the Siljan structure. Some of these observations, which may be relevant to the Deep Gas Project, are summarized below.

(i) Initial impact conditions are unknown. A reasonable assumption, however, is that the structure was the results of the impact of asteroidal-sized body in the size-range of a few kilometers. Impact energy was in range of 10^{22}J or greater and accompanying peak pressures were in the megabar range with temperatures close to the impact point in excess of the vaporization temperature of silicates.

(ii) Excavation was to a depth of several kilometers (~ 2.5 - 4.5 km), sufficient to penetrate through the Paleozoic sedimentary cover into the underlying Precambrian granites. Deep excavation was, however, limited to the central area now occupied by uplifted Dala granites.

(iii) Following excavation and large-scale modification associated with the impact, the final Siljan structure is estimated to have had a diameter of 52 km. It had a complex form with a central topographic peak and/or rings and a complexly faulted rim area. The preserved Paleozoic sediments were outside the area of deep excavation and represent down-faulted material from the interior of the final rim-area. The post-modification depth of the original structure may have been on the order of 1.5 km and the central structure(s) may have formed topographic peaks on the order of 1 km. These would have been surrounded by an overlapping annular sheet of impact melt rocks, possibly up to 200 m thick, extending out to the area of the Paleozoic sediments. Shock pressures recorded in the uplifted Dala granites were 25-30 GPa.

(iv) Post-impact shock heating in center was 100-200°C. This was in addition to the geothermal temperature of ~ 75°C associated with the uplift of the central granites from an original, pre-impact depth of 4-5 km. The post-shock temperature attenuated rapidly away from the center and was probably insignificant in the area of the Paleozoic sediments. Post-shock temperatures and those associated with the virtually instantaneous uplift of deep-seated rocks were supplemented by a thermal event associated with conductive cooling of the overlying melt. This thermal metamorphism was relatively local and confined to the volume of rock essentially in contact with the melt sheet. It is not known whether the melt sheet extended to the area of the Paleozoic sediments.

(v) Fracturing associated with the impact event was extensive, extending out to possibly 50 km beyond the original rim of Siljan. Major structural disturbances in the center are likely to have extended to depths of ~ 7 km, with the potential for increased, initial fracturing to lower crustal depths of 35-40 km. Many of these initial fractures may have been closed almost immediately by normal lithostatic pressure. In addition, many of the upper crustal fractures in the central area will have been closed by the inwards and upwards movement of material during the formation of the central uplift. This will have been supplemented by fracturing-healing due to hydrothermal deposition of minerals in the elevated temperature regime of the central uplift. Fracturing and faulting in the rim-area were not as deep-seated as in the center but are likely to have remained relatively open due to their location in an area of tension and low post-shock heating.

(vi) Erosion has since removed the topographic expression of Siljan, exposing and removing some of the original crater floor. Erosion for the area of the original rim and central structure(s) is estimated to have been on the order of ~ 1.5 and 1.0 km, respectively. The extent of erosion of the Paleozoic sediments is not known but may have been less, as they were initially in a relatively low topographic area.

(vii) Although not explicitly discussed, experience with recorded shock distribution and shatter cone orientations suggest that the center of the Siljan structure is expected to be at or near the geometric center of the annulus formed by the Paleozoic sediments. The suggestion by Wickman (1980) that the center is located 4-9 km north of the topographic center is based on a data-set of only four shatter cone localities with three of the localities lying within 90° of arc. In addition, shatter cone orientations at locality 2 (Wickman, 1980) differ from those reported from the same locality by Svensson and Robertson (pers. comm. in Wickman, 1980). If the Svensson and Robertson orientations for locality 2 are used in combination with Wickman's other data, the shatter cone "center" occurs ~ 5 km south of that suggested by Wickman (1980) and is closer to the geometric center. Given the limited data set and the complex nature of block movement during modification in the center of complex structures, there is insufficient evidence to call for an exceptionally off-center location in the case of Siljan.

REFERENCES

Barlow, B.C., 1979. Gravity investigations at the Gosses Bluff impact structure, Central Australia, Bur. Min. Res., Geol. and Geophys. 4, 323-339.

Bottomley, R.J., York, D. and Grieve, R.A.F., 1978. ^{40}Ar - ^{39}Ar ages of Scandinavian impact structures: I Mien and Siljan. Contrib. Mineral. Petrol., 68, 79-84.

Brennan, R.L., Peterson, B.L. and Smith, H.J., 1975. The origin of Red Wing Creek structure, McKenzie County, N. Dakota. Wyoming Geol. Assoc. Earth Sci. Bull., 8, No. 5, 41 p.

Brown, A.R., 1973. A detailed seismic study of Gosses Bluff, Northern Territory, Bur. Min. Res., Geol. and Geophys., Report 163, 43 p.

Cintala, M.J., 1984. A method for evaluating shock propogation and its thermal effects during impact events. Lunar Planet. Sci. XV, Lunar and Planetary Institute, Houston, TX, 154-155.

Cintala, M.J. and Grieve, R.A.F., 1984. Energy partitioning during terrestrial impact events: Melt production and scaling laws. Lunar Planet. Sci. XV, Lunar and Planetary Institute, Houston, TX, 156-157.

Croft, S.K., 1979. Impact craters from centimeters to magameters. Ph.D. thesis, Univ. Calif. Los Angeles, 264 p.

Croft, S.K., 1980. Cratering flow fields: Implications for the excavation and transient expansion stages of crater formation. Proc. Lunar Planet. Sci. Conf. 11th, 2347-2378.

Croft, S.K., 1984. The scaling of complex craters. Jour. Geophys. Res. (in press).

Dence, M.R., 1977. The Manicouagan impact structure, Quebec, from Skylab. In Skylab Explores the Earth, NASA SP-380, Washington, D.C., 175-190.

Dence, M.R., Grieve, R.A.F. and Robertson, P.B., 1977. Terrestrial impact structures: Principal characteristics and energy considerations. In Impact and Explosion Cratering (D.J. Roddy, R.O. Pepin and R.B. Merrill, eds.), Pergamon, New York, 247-275.

Dvorak, J. and Phillips, R.J., 1977. The nature of gravity anomalies associated with young large lunar craters. Geophys. Res. Lett., 4, 380-382.

French, B.M. and Short, N.M. (eds.), 1968. Shock Metamorphism of Natural Materials. Mono Book Corp. Baltimore, 644 p.

Gault, D.E., Quaide, W.L. and Oberbeck, V.R., 1968. Impact cratering mechanics and structures. In Shock Metamorphism of Natural Materials (B.M. French and N.M. Short, eds.), Mono Book Corp. Baltimore, 87-100.

Grady, D.E. and Hollenbach, 1979. Dynamic fracture strength of rock. Geophys. Res. Lett., 6, 73-76.

Grieve, R.A.F., 1982. The record of impact on earth: Implications for a major Cretaceous/Tertiary event. Geol. Soc. Amer. Sp. Paper 190, 25-38.

Grieve, R.A.F., 1984. The impact cratering rate in recent times. Jour. Geophys. Res., 89, Suppl., B403-B408.

Grieve, R.A.F. and Cintala, M.J., 1981. A method for estimating the initial impact conditions of terrestrial cratering events, exemplified by its application to Brent crater, Ontario. Proc. Lunar Planet. Sci. Conf. 12B, 1607-1621.

Grieve, R.A.F. and Garvin, J.B., 1984. A geometric model for excavation and modification at terrestrial simple impact craters. Jour. Geophys. Res. (in press).

Grieve, R.A.F. and Head, J.W., 1983. The Manicouagan impact structure: An analysis of its original dimensions and form. Jour. Geophys. Res., 88, Suppl., A807-A818.

Grieve, R.A.F. and Robertson, P.B., 1984. The potential for the disturbance of a buried nuclear waste vault by large-scale meteorite impact. Proc. Workshop on Transitional Processes, Atomic Energy Canada Limited, AECL - 7822, 231-260.

Grieve, R.A.F., Dence, M.R. and Robertson, P.B., 1977. Cratering processes as interpreted from the occurrence of impact melts. In Impact and Explosion Cratering (D.J. Roddy, R.O. Pepin and R.B. Merrill, eds.), Pergamon, New York, 791-814.

Grieve, R.A.F., Robertson, P.B. and Dence, M.R., 1981. Constraints on the formation of ring impact structures, based on terrestrial data. In Proc. Conf. Multi-Ring Basins, Pergamon, New York, 37-57.

Gurov, E.P. and Gurova, E.P., 1982. Some regularities of the areal spreading of fractures around Elgygytgyn crater. Lunar Planet. Sci. XIII, Lunar Planetary Institute, Houston, TX, 291-292.

Holsapple, K.A. and Schmidt, R.A., 1982. On the scaling of crater dimensions 2, impact processes. Jour. Geophys. Res., 87, 1849-1870.

Koglovsky, Y.A., 1982. Kola super-deep: Interim results and prospects. Episodes, 4, 9-12.

Masaitis, V.L., Danilin, A.N., Mashak, M.S., Raichlin, A.I., Selivanvskaya, T.V. and Shadyenkov, Y.M., 1980. The geology of Astroblemes (in Russian), Nedra, Moscow, 331 p.

Onorato, P.I.K., Uhlmann, D.R. and Simmonds, C.H., 1978. The thermal history of the Manicouagan impact melt sheet, Quebec. Jour. Geophys. Res., 83, 2789-2798.

Perrier, R. and Quiblier, J., 1974. Thickness changes in sedimentary layers during compaction history: Methods for quantative evolution. Amer. Assoc. Petrol. Geol. Bull., 58, 507-517.

Roddy, D.J., Pepin, R.O. and Merrill, R.B. (eds). Impact and Explosion Cratering, Pergamon, New York, 1301 p.

Rondot, J., 1975. Comparaison entre les astroblèmes de Siljan, Suède, et de Charlevoix, Québec. Bull. Geol. Instit. Univ. Uppsala, 6, 85-92.

Schultz, P.H. and Merrill, R.B. (eds.), 1981. Proc. Conf. Multi-Ring Basins, Pergamon, New York, 295 p.

Shoemaker, E.M., 1977. Astronomically observable crater-forming projectiles. In Impact and Explosion Cratering (D.J. Roddy, R.O. Pepin and R.B. Merrill, eds.), Pergamon, New York, 617-628.

Svensson, H.-B., 1971. Probable meteorite impact crater in central Sweden. Nature, 229, 90-92.

Svensson, N.-B., 1973. Shatter cones from the Siljan structure, central Sweden. Geol. Foreningens i Stockholm Forhandlin-gar, 95, 137-143.

Sweeney, J.F., 1978. Gravity study of great impact. Jour. Geophys. Res., 83, 2809-2815.

Wickman, F.E., 1980. The impact center of the Siljan structure, central Sweden. Geol. Foreningens i Stockholm Forhandlin-gar, 102, pt. 2, 105-109.

FIGURE CAPTIONS

Figure 1 Geologic sketch map of Siljan ring structure, from Bottemley *et al.* (1978).

Figure 2 Schematic diagram illustrating the formation of a complex structure such as Siljan, from Grieve *et al*. (1981). Excavation/compression stage - maximum growth of the excavated (EC) and transient cavities (TC). Shaded region depicts flow field configuration of melted and brecciated material beneath maximum penetration of meteorite. Dashed envelopes illustrate ejection trajectories from a series of earlier, transitional stages in cavity growth, and are a first-order approximation of cavity shape at these times. Uplift (excavation) stage - maximum rebound of transient cavity floor above regional surface. Excavation may continue with material driven outward over cavity rim in turbulent flow producing secondary removal of surface material beyond D_e. Collapse stage - overheightened, physically unstable uplift collapses with overthrusting and stacking of strata. Excess volume is accommodated in topographic ring peaks on flanks at approximately D_e. Breccia (and impact melt) accumulates on flanks of uplift and in peripheral depression. Final form - Central uplift collapses to below original surface. Outer rim is produced by downfaulting, further deepening the peripheral depression. Limit of intense brecciation and faulting shown by dashed envelope.

Figure 3 Red Wing Creek, N. Dakota - an example of a complex impact structure in sedimentary rocks. A cross-section of present morphology and structure from drilling (8 vertical lines) and seismic data, illustrates stratigraphic uplift (SU) of Mississippian and disturbance as deep as the Devonian (D). The Permian Minnekahta Formation is depicted immediately below the crater surface in the peripheral trough region. The margin of the final crater (D_a) is marked by steep, normal faults. Structure is largely preserved under Jurassic (J) and Cretaceous (K) post-crater sediments. Reconstruction of the excavated cavity indicates deep central excavation within D_e and shallow removal of strata to D_a. From Grieve _et_ _al_. (1981).

Figure 4 Depth/diameter relationships (solid lines) and structural uplift (broken line) at terrestial craters. Structures in sedimentary targets develop complex form at smaller diameters than those in crystalline targets, reflecting the physical properties of target. Physical heights of central uplifts or rings (closed symbols) never exceed final crater depth, indicating final height (depth) is equilibrium feature. Amount of structural uplift (open symbols) increases with diameter. U is equivalent to SU in text.

Figure 5: (a) Location of gravity profiles across Manicouagan shown in Figure 5b.

(b) Residual Bouguer gravity profiles, after removal of regional field, associated with the Manicouagan structure. Profiles constructed from Figure 5 in Sweeney (1978). The minimum gravity values are in the area of the annular moat, which is structurally equivalent to the area of Paleozoic sediments at Siljan.

APPENDIX:

Summary of petrographic observations from drill-hole samples

Hole 1, Depth 378 m

Altered granite, fractured but not brecciated. Fractures unfilled but relatively tight.

Mineralogy

~ 75%	Subhedral feldspar up to 5 mm in size. Heavily altered to kaolin. Both plagioclase and alkali feldspar present.
~ 25%	Anhedral, interstitial quartz, generally 1-2 mm in size and showing strained extinction. Accessory amounts of chloritized biotite.

Hole 2, Depth 126 m

Brecciated granite, heavily fractured with fractures filled by calcite and/or chlorite. Mineral fragments up to 10 mm are angular to sub-rounded and set in a clastic matrix of the same components.

Mineralogy

~ 30%	Plagioclase.
~ 30%	Microcline. Both moderately altered to white mica and/or kaolin.
~ 20%	Quartz with strained extinction. Level of deformation higher than in Hole 1, 378 m, showing Bohm lamellae but no unequivocal shock planar features.
~ 7%	Calcite, generally occurring as a fracture filling product.
~ 5%	White mica.
~ 5%	Chloritized biotite.
~ 3%	Chlorite.

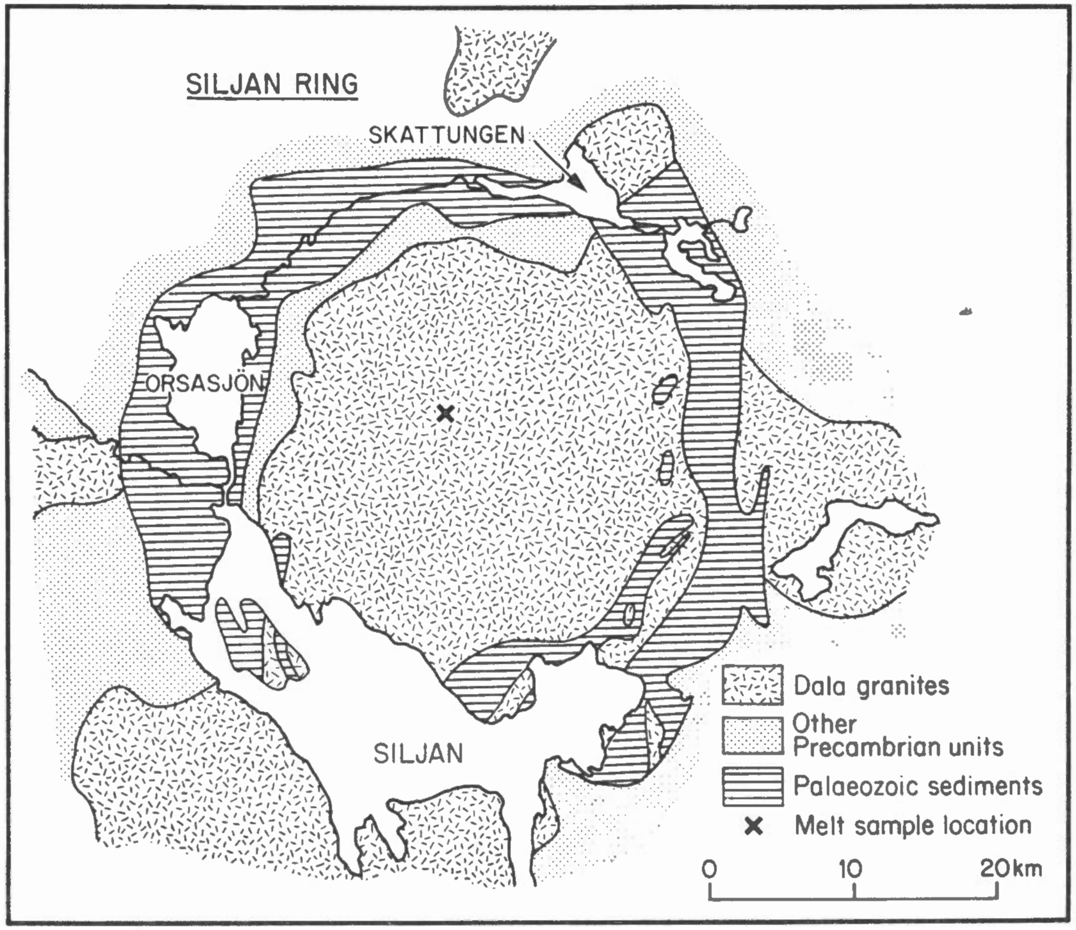

Fig. 1. Siljan as an impact structure

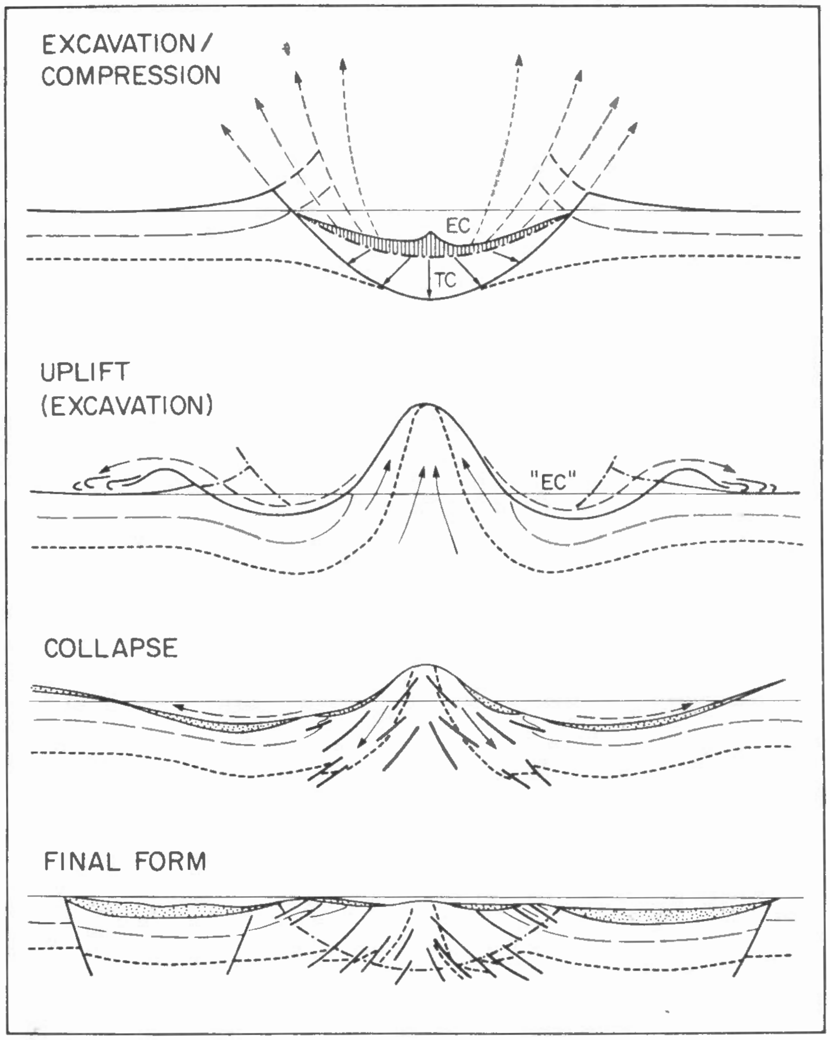

Fig. 2. Siljan as an impact structure.

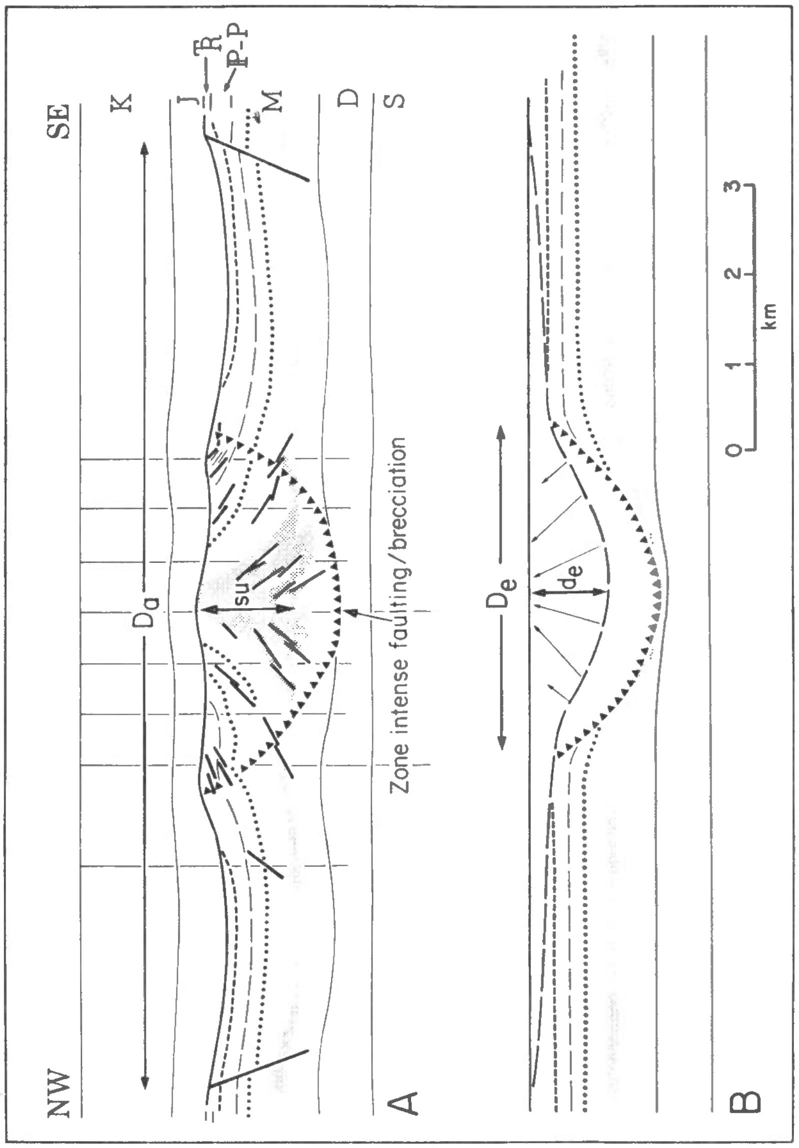

Fig 3. Siljan as an impact structure.

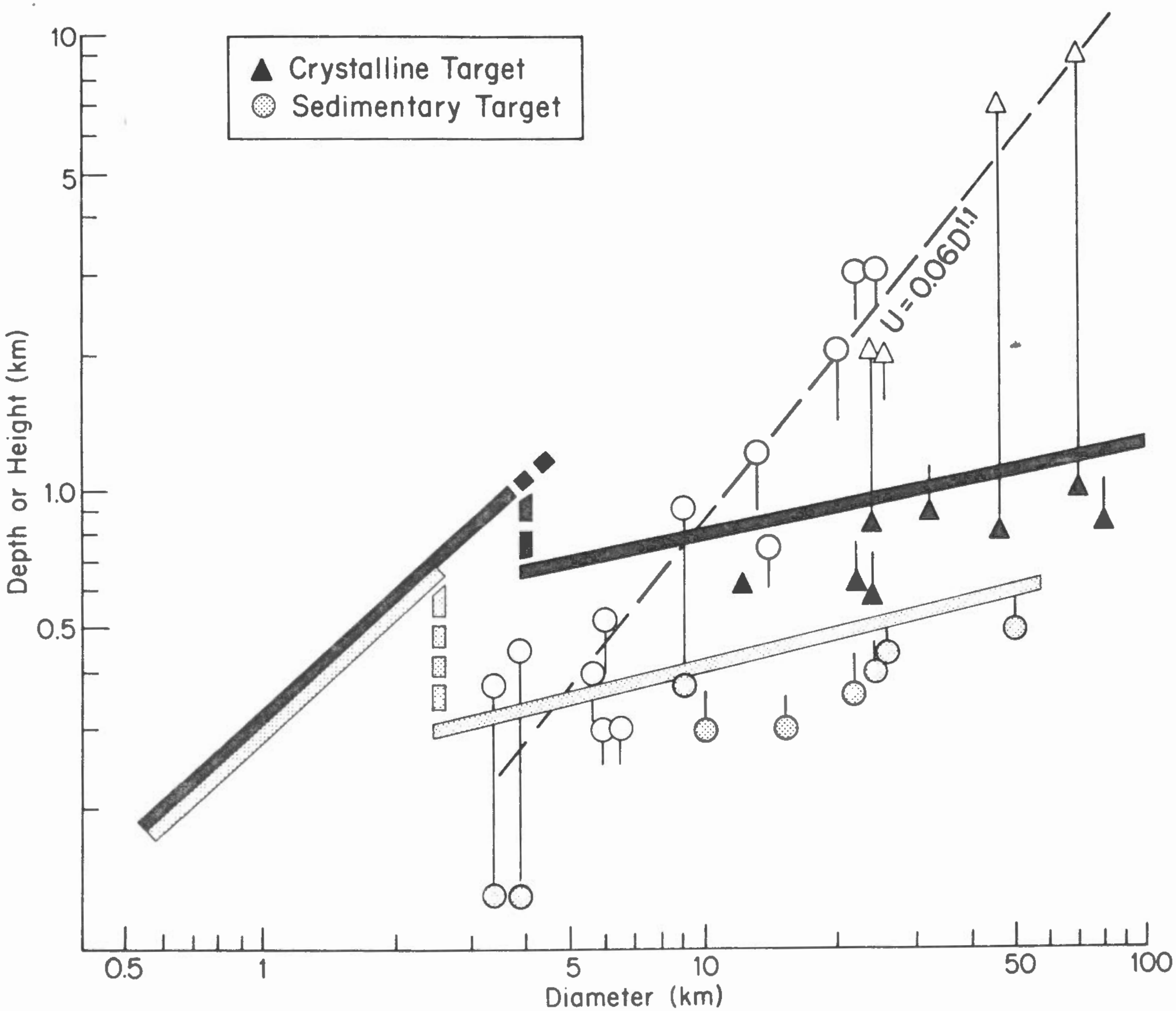

Fig 4. Siljan as an impact structure

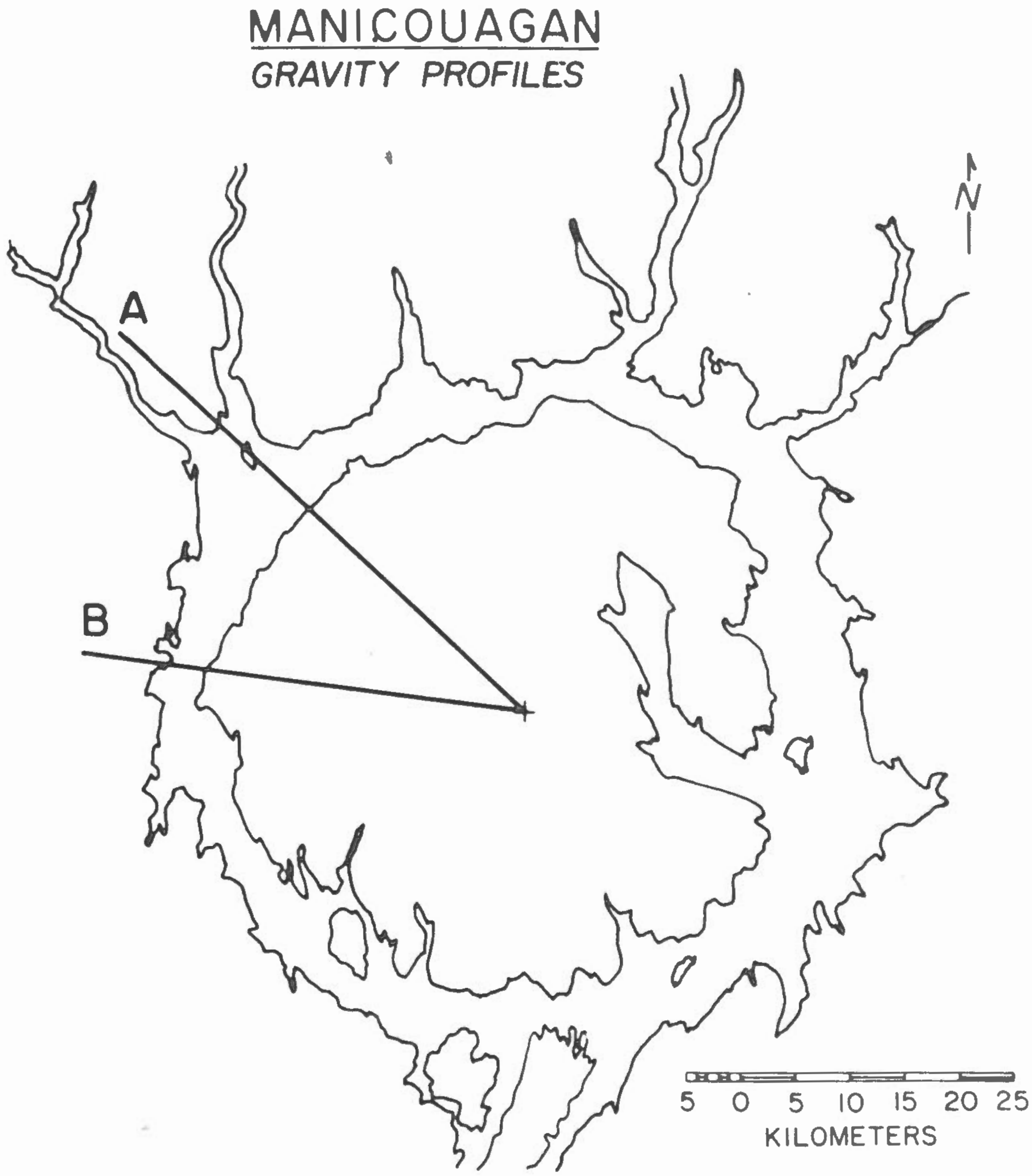

Fig 5a. Siljan as an impact structure

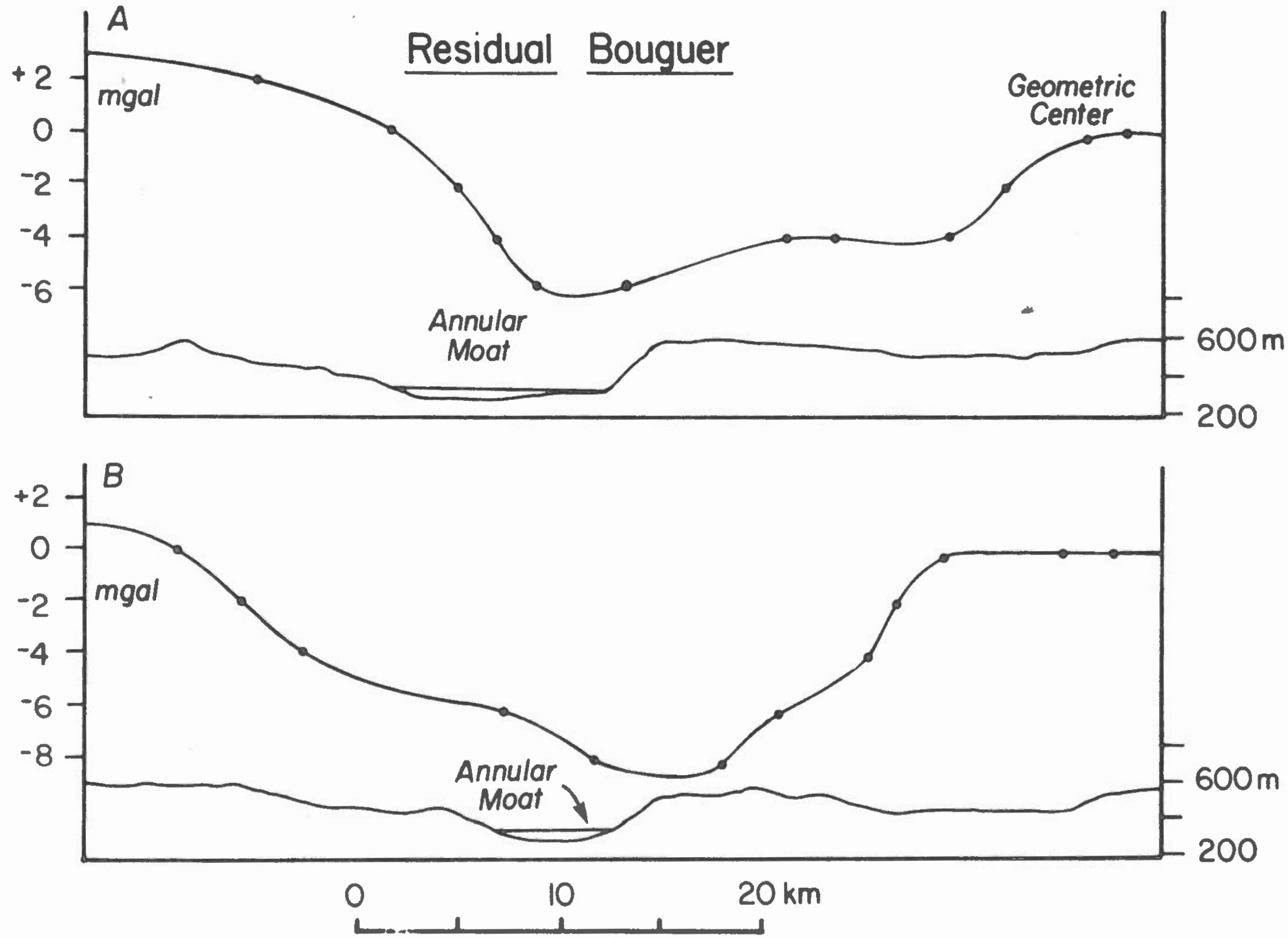

Figure 86. Siljan as an impact structure.